Widely tunable optical nanocavity photonic crystal sensor

Soon Thor Lim, Ching Eng Png
Advanced Photonics and Plasmonics
IHPC, A*Star
Singapore
limst@ihpc.a-star.edu.sg

Maoqing Xin, Aaron Danner
Dept. of Electrical and Computer Engineering
National University of Singapore
Singapore
adanner@nus.edu.sg

Abstract— **A large peak shift of 12 nm is reported from a silicon-on-insulator waveguide with photonic crystal filter. With high Q and 10dB modulation depth, fast and accurate sensing may be possible.**

Keywords-photonic bandgap, sensing, modulators

I. INTRODUCTION

Optical sensing often relies on the detection of a small change in refractive index, usually caused by a fluid or gas passing through an optical resonator, or a small change in absorption. Photonic crystals-based sensors are often plagued by the inability to fabricate photonic crystals with resonance peaks that are reproducible run-to-run. In this presentation, we show that adding a small amount of electrical tunability (with low power consumption) can both allow active correction for fabrication errors—a sort of way to calibrate away fabrication errors—and allow sensing at multiple wavelengths or even to scan through a series of wavelengths. With as much as a 12 nm tuning range for a single resonator, multiple resonators could be arrayed to achieve broadband tunability.

II. DEVICE CONFIGURATION

Fig. 1 shows an optical nanocavity sensing device that can be scalable to include array of sensors that are formed by photonic bandgap structures. Although a passive device is shown, active devices could just as easily be incorporated into the device as will be described. Two possible structures are discussed; first a one dimensional (1-D) periodic air hole similar to [1-2], where the local defect inside the photonic crystal leads to highly confined optical states, such structure are optimized for large peak shift with low power consumption. Second, a cross waveguide resonator, where two identical one dimensional (1D) subwavelength Fabry –Perot (FP) waveguide resonators [3] are configured perpendicular to each other to form a microcavity at the central intersection, therefore optimized for device speed through a more efficient carrier injection scheme as compared to a single FP waveguide resonator approach.

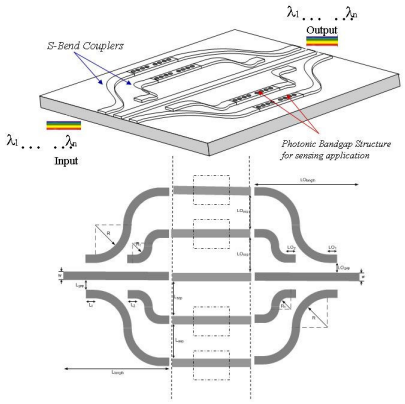

Fig. 1 Schematic diagram of a passive nanocavity sensor suitable for multiple sensing applications

III. 1-D PHOTONIC BANDGAP FOR OPTIMIZED PEAK SHIFT

An optical nanocavity is configured by using a rib waveguide of 470 nm width and an optimized etch depth of 180 nm with an ultra-thin silicon slab layer of 23 nm as shown in Fig. 2 with five etching air-holes on both sides of the structure creating a central defects. Such configuration reduces the doping volume and more significantly, reduces the total number of injected free carriers, whilst maintaining sufficient modal overlap thus allows the reduction in power consumption without sacrificing the modulation depth. The device is a two terminal *p-i-n* structure where both *n* and *p* regions were modeled using ATLAS device simulation package from SILVACO, as highly doped regions with constant doping concentrations of 10^{20} cm^{-3}.

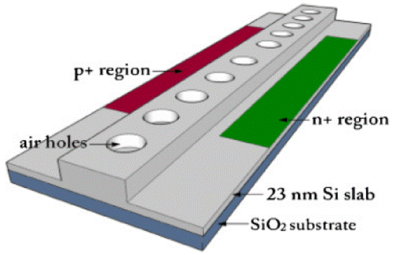

Fig. 2 3D schematic of 1D photonic bandgap nanocavity with p+ and n+ doping region

The device is biased at various voltage points as shown in Fig. 3. It can be noted that the rise and fall times are approximately 6.2 ns and 3.8 ns which is suitable for fiber to the home (FTTH) and sensing applications. The level of carrier concentration is converted to its equivalent optical properties, e.g. refractive index change and absorption coefficient for optical characterization. Fig. 4 shows the relationship of power density between resonance peak-shift and modulation depth, where the power density, P_{DC} is defined as:

$$P_{DC} = V_{bias} I \quad (1)$$

where V_{bias} is the bias voltage and i is the current density. Therefore, from figs. 3 and 4, a 10dB modulation depth at a power of 186 µW/µm with a large peak shift of 12nm is expected. This peak shift is an order of magnitude larger than what was reported in [4].

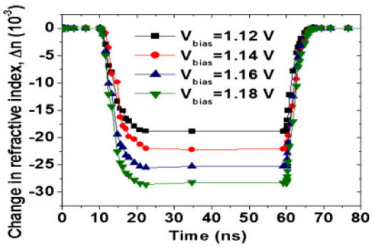

Fig 3 Transient characteristic of the photonic bandgap at different bias voltages.

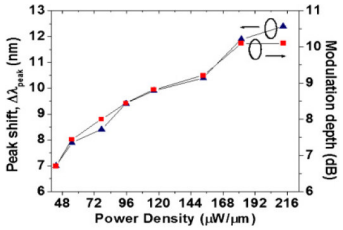

Fig. 4 Relationship between resonance peak shift, modulation depth and power density

IV. CROSS WAVEGUIDE RESONATOR FOR OPTIMIZED DEVICE SPEED

Alternative configuration for optimized device speed can be achieved by creating an optical nanocavity at the intersection of two identical 1D photonic bandgap structures know as a cross waveguide resonator. A localized transverse-electric (TE) mode is allowed due to the central defects of the 1D photonic bandgap and the two opposite branches are partially doped with p+ and n+ regions so that a transverse p-i-n diode is embedded into the cross waveguide as shown in fig. 5. It can be observed from fig. 6 that the bias voltage and the drive current decrease with increasing carrier concentration, hence allowing the same modulation depth with a lower power consumption. However, optical absorption increases with increased dopant concentration. At a concentration level of 4 x 10^{19} cm^{-3}, the optical loss is at 1.68 dB. The transient refractive index change of the nanocavity is shown in fig. 7. The voltage is varied from 1.22V to 1.8V. A modulation speed of 2.9 GHz is expected when the bias voltage is at 1.65V, DC power consumption of 17.3 mW, with a 3dB frequency around 4 GHz.

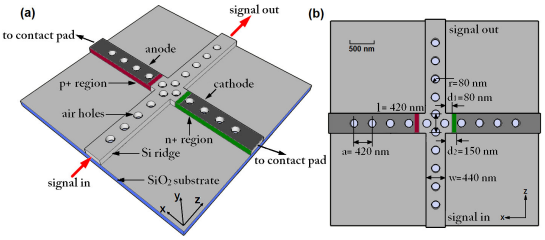

Fig. 5 (a) 3D schematic of the cross waveguide resonator based modulator; (b) top view of the device with notations of the optimum device dimensions.

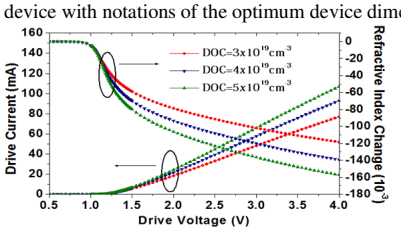

Fig. 6 I-V characteristics of the p-i-n diode shows a lower bias voltage is needed to achieve the same RI change for higher doping concentrations

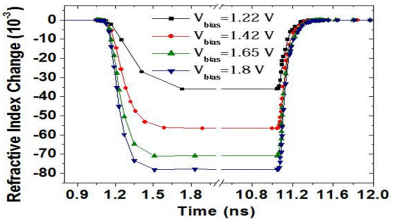

Fig. 7 DC and transient characteristics of the device performance: the relationship between modulation depth, peak shift and power consumption

V. CONCLUSIONS

Our results suggest that very small photonic crystal structures can be placed in an arrayed on-chip environment for broadband active sensing.

ACKNOWLEDGMENTS

A research grant from Singapore's Ministry of Education is acknowledged.

REFERENCES

[1] J. S. Foresi, P. R. Villeneuve, J. Ferrera, E. R. Thoen, G. Steinmeyer, S. Fan, J. D. Joannopoulos, L. C. Kimerling, H. I. Smith, and E. P. Ippen, "Phonotic-bandgap mocrocavities in optical waveguides," *Nature*, vol. 390, pp. 143-145, 1997.

[2] C. E. Png, S. T. Lim, E. P. Li, and Graham. T. Reed, "Tunable and sensitive biophotonic waveguides based on photonic-bandgap microcavities," *IEEE Trans. on NanoTechnol,*. vol. 5, no. 5, pp 478-484, 2006.

[3] N. Moll, R. Harbers, R. F. Mahrt, and G.-L. Bona, "Integrated all-optical switch in a cross-waveguide geometry," Appl. Phys. Lett., vol. 88, 171104, 2006.

[4] B. Schmidt, Q. Xu, J. Shakya, S. Manipatruni, and M. Lipson, "Compact electro-optic modulator on silicon-on-insulator substrates using cavities with ultra small modal volumes", *Optics Express*, vol. 15, no. 6, pp. 3140-3148, 2007.